SCIENTIFIC REPORTS

OPEN

SUBJECT AREAS:
STRUCTURAL BIOLOGY
CANCER METABOLISM

Received
9 October 2013

Accepted
3 January 2014

Published
23 January 2014

Correspondence and requests for materials should be addressed to J.S. (dbsjayar@nus.edu.sg)

Structural Basis for the Active Site Inhibition Mechanism of Human Kidney-Type Glutaminase (KGA)

K. Thangavelu[1], Qing Yun Chong[1], Boon Chuan Low[1,2] & J. Sivaraman[1]

[1]Department of Biological Sciences, 14 Science Drive 4, National University of Singapore, Singapore 117543, [2]Mechanobiology Institute Singapore, National University of Singapore, Singapore 117411.

Glutaminase is a metabolic enzyme responsible for glutaminolysis, a process harnessed by cancer cells to feed their accelerated growth and proliferation. Among the glutaminase isoforms, human kidney-type glutaminase (KGA) is often upregulated in cancer and is thus touted as an attractive drug target. Here we report the active site inhibition mechanism of KGA through the crystal structure of the catalytic domain of KGA (cKGA) in complex with 6-diazo-5-oxo-L-norleucine (DON), a substrate analogue of glutamine. DON covalently binds with the active site Ser286 and interacts with residues such as Tyr249, Asn335, Glu381, Asn388, Tyr414, Tyr466 and Val484. The nucleophilic attack of Ser286 sidechain on DON releases the diazo group (N_2) from the inhibitor and results in the formation of an enzyme-inhibitor complex. Mutational studies confirmed the key role of these residues in the activity of KGA. This study will be important in the development of KGA active site inhibitors for therapeutic interventions.

Besides aerobic glycolysis, or the Warburg effect, the involvement of glutaminolysis in cancers has received increasing attention as a potential avenue for the development of new therapeutic agents for cancer treatment[1]. Glutaminase controls the first step in the glutaminolysis pathway by converting glutamine (Gln) to glutamate (Glu), with subsequent enzymatic reactions generating aspartate, malate, pyruvate, citrate, alanine, and lactate[2]. It has been widely accepted that cancer cells favour glutamine as a source of energy, and this phenomenon has been observed in many cancers[3,4]. Thus, various studies postulate that inhibiting glutaminolysis by preventing the activity of this key enzyme would significantly hinder cancer cell growth and proliferation. Consequently, glutaminase has become an intriguing target for the development of drugs against human cancers[5–8].

To date, three isoforms of human glutaminase have been identified: kidney-type (KGA/GLS1), the splice KGA variant (Glutaminase C or GAC), and liver-type (LGA/GLS2)[9,10]. Gao et al. recently showed that c-Myc stimulates KGA expression in P493 human B lymphoma and PC3 prostate cancer cells through direct suppression of miR23a and miR23b[6]. Similarly, activation of transforming growth factor beta (TGF-β) has been shown to stimulate KGA expression[11]. Importantly, the small GTPase, Rho, a pro-oncogenic molecule, can up-regulate KGA activity[7], and we recently showed that KGA activity can be regulated by the Ras/Raf/Mek/Erk signalling cascade in response to growth factor stimulation[8]. Moreover, LGA was reported to be regulated by p53 in the energy producing-glutaminolysis pathway[12,13]. Collectively, these observations indicate that targeting KGA-mediated glutaminolysis could have high therapeutic implications with which to control cancer.

The glutamine analogue, 6-diazo-5-oxo-L-norlucine (DON), inhibits KGA and its isoforms by binding to the active site[14]. DON is a diazo compound and is known to interfere with both nucleotide and protein synthetic pathways where glutamine acts as a substrate[15]. However, DON lacks selectivity, as it also inhibits other glutamine-utilising enzymes such as the amidotransferases and glutamine synthetase[16,17]. The potential anti-cancer activity of DON was previously investigated in different animal models; however, concerns surrounding its toxicity prohibited its progression into clinical trials[18,19]. Similarly, a glutamate analogue, CK (L-2-amino-4-oxo-5- chloropentanoic acid), was also previously reported to act at the active site of KGA[20] but was also not further explored. The recent renewed interest in cancer metabolism has raised the possibility that the optimization and systematic use of DON may have profound effects on human cancers.

The crystal structure of glutaminase from *E.coli* and *B. subtilis* in complex with DON has revealed the key role of a serine residue as a catalytic nucleophile[21]. We recently reported the crystal structure of the catalytic domain of kidney-type glutaminase (cKGA) in complex with L-glutamine and L-glutamate and proposed a catalytic

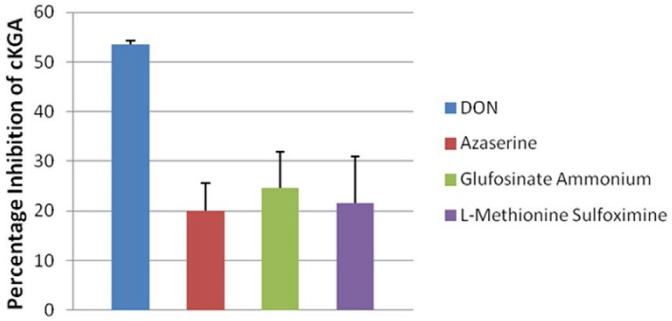

Figure 1 | Comparison of the relative inhibition percentage of cKGA by selected glutamine/glutamate analogues at 1 mM concentration (IC_{50} of DON is approximately 1 mM). The assays were performed in triplicates and values are mean ± SD of three independent experiments.

mechanism for KGA[8]. The catalytic dyad of KGA consists of Ser286 and Lys289 (286-SCVK-289), and confirmed previous findings that the Ser286 acts as a catalytic nucleophile. In addition, we and others have reported the existence of a novel allosteric switch that governs the inhibition mechanism of KGA and GAC isoforms by BPTES[8,22]. Subsequently, Cassaga et al. proposed the activation mechanism of the GAC isoform by solving its crystal structure in complex with phosphate[23].

To date, there have been no structural studies reported for any of the human glutaminase isoforms (KGA or GAC, LGA) in complex with their active site inhibitors. Here, we report the active site inhibition studies of KGA with several putative active site inhibitors as well as the crystal structure of cKGA in complex with DON. Similar to bacterial glutaminase, we show that DON forms a covalent bond with the active site Ser286 residue of KGA. Further, using site-directed mutagenesis, we validated the importance of various key residues involved in these interactions with DON. Taken together, these studies form the basis of a strategy to optimise KGA active site inhibitors for the improved and selective inhibition of this enzyme and may thus offer a first step toward the development of therapeutic intervention against glutamine-dependent cancers.

Results

Active site inhibition of cKGA by substrate analogue inhibitors. DON and azaserine are glutamine analogues that are known to inactivate several glutamine-utilising enzymes, such as glutaminase, amidotransferases and glutamine synthetase[24]. Besides, two additional glutamate analogues–glufosinate ammonium and L-methionine sulfoximine–were previously shown to inhibit the activity of glutamate-dependent enzymes[25,26]. We first conducted assays to identify which of these four inhibitors could best inhibit the activity of KGA (Figure 1). We found that DON inhibited cKGA significantly better than the other three inhibitors, with an IC_{50} of approximately 1 mM (Figure 1). Thus, DON was used in subsequent experiments to study the active site inhibition mechanism of KGA.

Structure of cKGA: DON complex. Molecular replacement method, using coordinates derived from *apo* cKGA (PDB code 3voy), was used to solve the cKGA: DON complex. The final model was refined with good stereochemical parameters (Figure 2A, Table 1). The complex structure of cKGA: DON shows that the inhibitor forms a covalent bond with the side-chain hydroxyl (OH) group of the catalytic nucleophile Ser286 (1.4 Å). This was confirmed by the continuous electron density from the active-site residue Ser286 with the inhibitor (Figure 2B). This Ser286 residue is conserved among all KGA isoforms. Using a one-to-one comparison based on the superposition of cKGA: DON and the *apo*-cKGA (rmsd of 0.3 Å for 315 Cα atoms), we observed no significant structural changes in cKGA upon its interaction with DON (Figure 3).

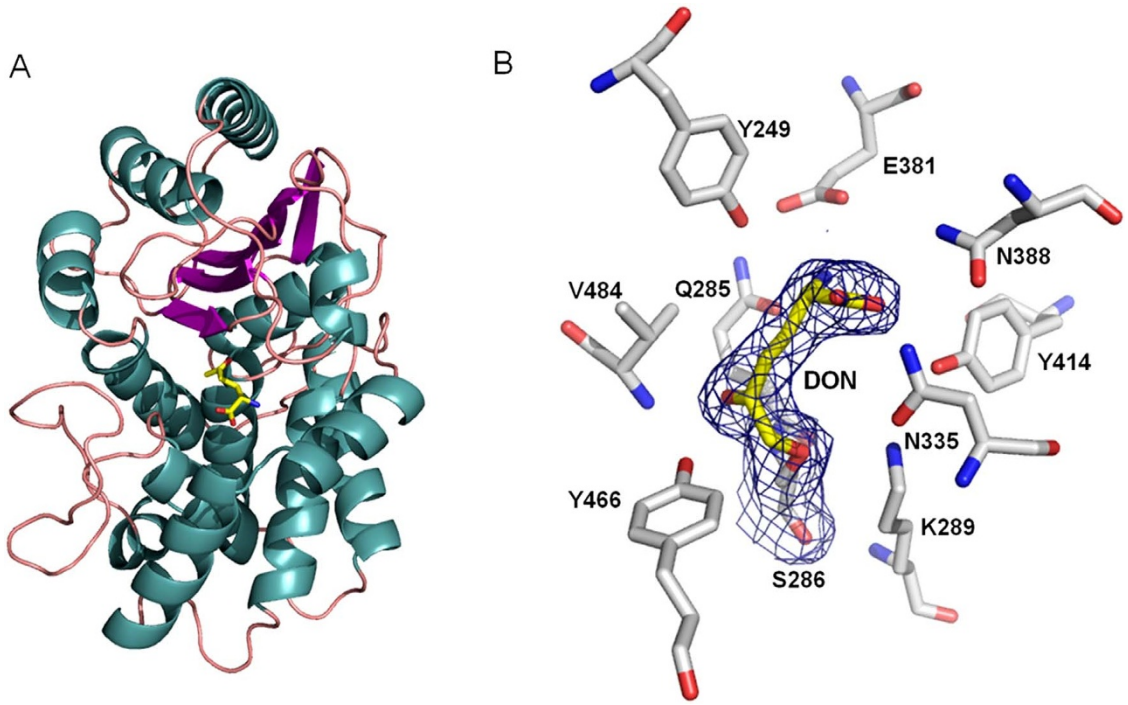

Figure 2 | Structure of cKGA: DON complex. (A) Ribbon representation of the cKGA: DON complex. Secondary structures α-helices and β-sheets are shown in dark green and magenta, respectively. DON is located in the active site cleft and is shown as a yellow stick. (B) Interactions made by DON in the catalytic pocket of cKGA. DON is shown in yellow and cKGA residues are shown in grey. Final *2Fo-Fc* electron density map for DON and its covalent attachment to Ser286 of cKGA is shown. The map is contoured at σ level of 1.0. This figure and other structure-related figures reported in this paper were prepared using Pymol[39].

Table 1 | Crystallographic data and refinement statistics for cKGA: DON complex

	Data Collection cKGA: DON complex
Space group	$I4_122$
Cell parameters (Å, °)	A = 139.27,b = 139.27, c = 156.50, α = β = γ = 90
Resolution range (Å)	30–2.3 (2.34–2.30)
Wavelength (A)	1.000
Observed *hkl*	392469
Unique *hkl*	34102
Completeness (%)	99.6 (95.7)
Overall $I/\sigma I$	12.7
[a]R_{sym}	0.054 (0.392)
Refinement and quality of the model	
*Resolution range (Å)	25.7–2.30
[b]Rwork (%) no. reflections	19.28 (23221)
[c]Rfree (%) no. reflections	21.08 (1722)
Root mean square deviation	
Bond length (Å)	0.007
Bond angle (°)	1.02
Ramachandran plot (%)	
Favored region	88.1
Allowed regions	11.2
Generously allowed region	0.7
Disallowed regions	0
Average B-factors (Å²)	
Main chain atoms	52.04
Side chain atoms	57.43
Overall protein atoms (no. atoms)	54.63 (2412)
Waters (no. atoms)	54.63 (89)
Ligand (no. atoms)	53.26 (10)

[a]$R_{sym} = |I_i - \langle I \rangle| / |I_i|$ where I_i is the intensity of the i^{th} measurement, and $\langle I \rangle$ is the mean intensity for that reflection.
[b]$R_{work} = |F_{obs} - F_{calc}| / |F_{obs}|$ where F_{calc} and F_{obs} are the calculated and observed structure factor amplitudes respectively.
[c]R_{free} is as for R_{work}, but only for 5% of the total reflections chosen at random and omitted from refinement.
*The high resolution bin details are in the parenthesis.

cKGA: DON interactions. The complex structure of cKGA: DON shows that the inhibitor binds in the catalytic pocket. The nucleophilic attack of the Ser286 side-chain on DON releases the diazo group (N_2) from DON in the complex, thereby covalently connecting the enzyme with the 5-oxo-l-norleucine (ON) component of the inhibitor to form a stable cKGA-ON complex (Figure 6). The bound inhibitor maintains several hydrogen bonding and hydrophobic interactions with Tyr249, Gln285, Ser286, Asn335, Glu381, Asn388, Tyr414, Tyr466, and Val484 of cKGA (Figure 2B). In particular, the carbonyl oxygen of the inhibitor is involved in two hydrogen-bonding contacts with the backbone amino (NH) group of Ser286 and Val484, and forms an oxyanione hole. Similarly, the α-carboxyl oxygens of the inhibitor are involved in two hydrogen-bonding contacts with the side-chains of Asn335 and Tyr414 of the enzyme. Moreover, the backbone NH group of the inhibitor is involved in a hydrogen bonding contact with the side-chains of Gln285 and Glu381 (Table 2). Besides these interactions, a hydrophobic cluster, formed by the side-chains of Tyr249, Tyr414 and Tyr466, further stabilises the interaction between cKGA and DON (Figure 2B). Notably, Tyr466 is located close to DON (3.2 Å) and also close to the catalytic Ser286 (2.7 Å), which is responsible for the proton transfer during catalysis. Previously, we proposed that Tyr466 played a key role in the catalytic mechanism along with the active site dyad (Ser286- CV-Lys289)[8]. The electrostatic surface potential of the cKGA: DON complex shows a predominantly positively charged active site region (Figure 4), with major contributions from the neighbouring residues (Lys299 and Lys491) of the active site region of cKGA.

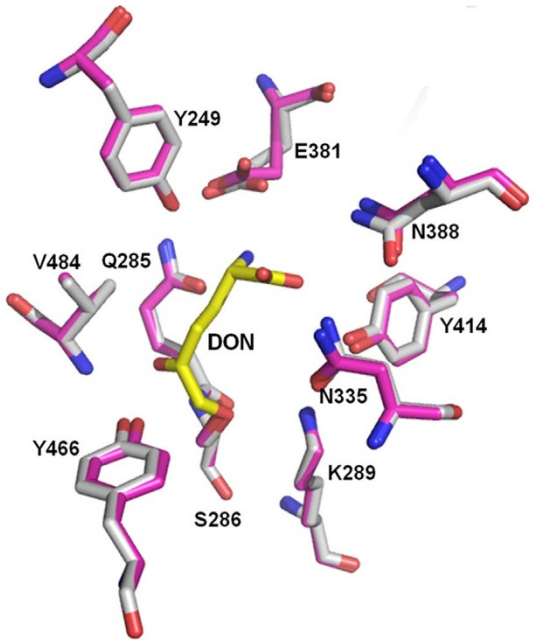

Figure 3 | Crystal structure of *apo* cKGA superimposed with cKGA: DON. The active site residues of *apo* cKGA and cKGA: DON is shown in magenta and grey, respectively.

Mutational studies at the cKGA active site region. The complex structure of cKGA: DON revealed the key residues from cKGA that are essential for its interaction with DON. To validate the role of these key interacting residues of KGA in its enzymatic activity, we generated several alanine substitution mutants and measured their activities using a glutaminase assay. We found a significant reduction in the activity of cKGA mutants Tyr249A, Ser286A, Lys289A and Tyr466A as compared with the wild-type cKGA (Figure 5), which greatly affected substrate binding. Thus, our study confirms that the putative catalytic dyad Ser 289-CV-Lys289 and other residues, such as Tyr249 and Tyr466, play key roles in the activity of KGA.

Inhibition of KGA by DON. The cKGA: DON complex structure shows that DON is bound to the active site of KGA through covalent modification of the Ser286 residue. Based on our observations and previous literature, we propose a mechanism for the active site inhibition of KGA by DON (Figure 6). First, a hydroxyl proton from the active site Ser286 residue is donated to the diazo ketone of DON, resulting in the formation of the diazonium ion. Next, the nucleophilic attack of the Ser side-chain oxygen (Oγ) on the inhibitor releases N_2 from the inhibitor. This is follwed by the generation of covalent linkage between Ser286 and the inhibitor, thus forming a stable enzyme-inhibitor complex. In our crystal strcture, we observed that the hydroxy oxygen of Ser286 is positioned about 1.4 Å from the δ carbon of DON. Based on this complex structure, it can be

Table 2 | Hydrogen bonds (Å) formed by DON in the active site of cKGA

DON atom	cKGA atom	Distance (Å)
O5	Ser286N	2.98
O5	Val484N	2.82
O1	Asn335ND2	3.13
O5	Tyr466OH	3.25
NH	Gln285OE1	2.79
NH	Glu381OE2	2.85
O5	Tyr249OH	3.24
O1	Tyr414OH	2.84

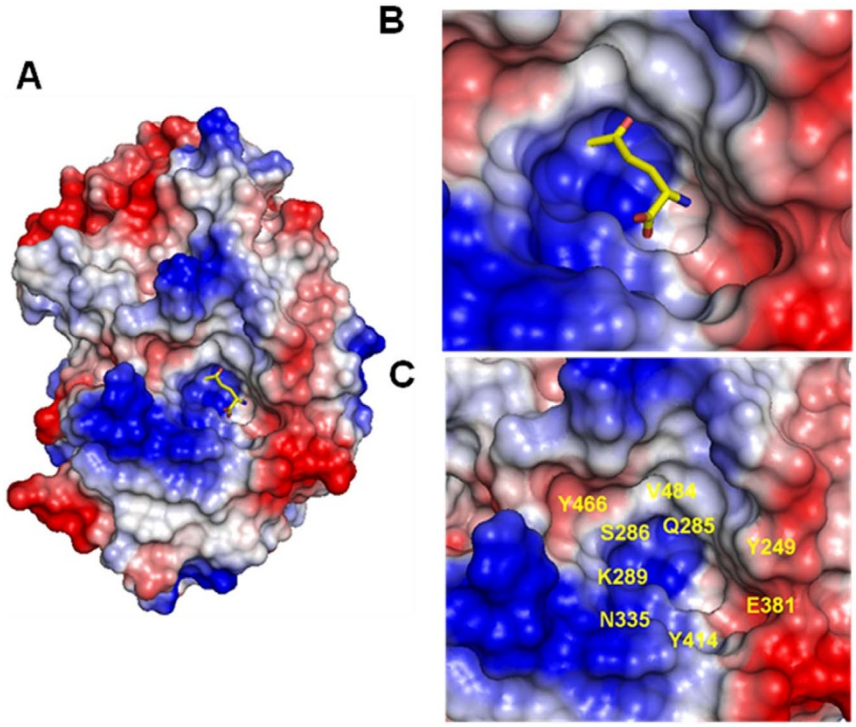

Figure 4 | Binding pocket of DON in cKGA. (A) Shows the electrostatic surface potential of cKGA: DON complex. DON is shown as a yellow stick. (B) A close-up view of the electrostatic surface potential shows a positively charged pocket around DON. (C) The residues that interact with DON in the active site cleft are labeled.

proposed that Lys289 of KGA acts as a general base to assist the catalytic Ser286 residue, and this is further supported by a side-chain hydroxyl oxygen of Tyr 466. Moreover, the sequence conservation and structural homology between KGA and its homologues (e.g., glutaminase from *E. coli* and *B. subtils*) suggest a common mode of the active site inhibition mechanism[21].

The superposition of cKGA: DON with YbgJ: DON (PDB code: 3BRM) gave a root mean square deviation (RMSD) of 1.3 Å for 285 Cα atoms. The cKGA has 36% sequence identity with its homologue YbgJ from *B. subtilis*. The active site residues of these two complex structures were well aligned, suggesting that human KGA may utilize similar catalytic mechanisms as its bacterial homolog (Figure 7A). Moreover, the superposition of cKGA: DON complex with cKGA: Glutamine (PDB code: 3VPO) gave a RMSD of 0.3 Å for 312 Cα atoms. Although the active site of both structures was identical, subtle differences in the position of bound DON in the active site can be observed (Figure 7B).

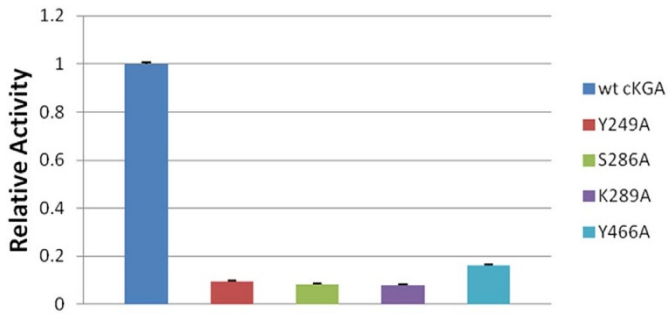

Figure 5 | Activities of wild-type cKGA compared with structure-guided cKGA alanine mutants. Triplicate datasets were obtained for each of the cKGA constructs. Values are mean ± SD of three independent experiments.

Discussion

Recent studies have highlighted the importance of KGA as a promising molecular target for various human cancers[5–8,22,23]. Notably, small molecule anti-cancer inhibitors targeting KGA are in the early stage of clinical testing[27]; the success of these potential inhibitors, however, will require a clear understanding of the molecular mechanism of KGA inhibition. The current renewed interest in cancer metabolism raises the possibility that systematic treatment with DON, or another small molecule inhibitor, may be beneficial against human cancers.

In our studies, we found that DON significantly inhibits KGA at an approximate IC_{50} of 1 mM. Similarly, 2–10 mM DON can inhibit bacterial glutaminase (YbaS), although it acts as a covalent inhibitor[21]. A similar concentration range was reported for the covalent inhibition of human cystathionine gamma-lyase by DAG, which acts at an IC_{50} of 0.2 mM[28]. Moreover, several studies have reported the weak, irreversible, and time-dependent inhibition mode of DON on glutaminase[14,29–31]. Whereas DON has been used widely to understand the functional role of KGA and other glutaminase isoforms, the lack of potency and selectivity of the compound has hindered its use in therapeutics. Hence, it is necessary to optimise the specificity of DON towards KGA for it to be a relevant option. The structure of the human cKGA: DON complex provides insight into the mode of binding and its activity, which will be important for the optimization, design and synthesis of a new series of DON analogues. In addition, BPTES and compound 968 (a dibenzophenanthridine) were recently identified as allosteric inhibitors of KGA and shown to block cancer cell growth and proliferation[5,7,8]. We recently elucidated the mechanism of allosteric inhibition of KGA by BPTES, showing that BPTES binds to KGA at the dimeric interface near the active site, and destabilises the activity of enzyme through a drastic conformational change in a key loop (Glu312-Pro329)[8]. We further showed that alanine substitutions in this allosteric loop caused a reduction in the enzymatic activity as compared with wild-type, suggesting that the BPTES binding loop residues are essential for conferring KGA

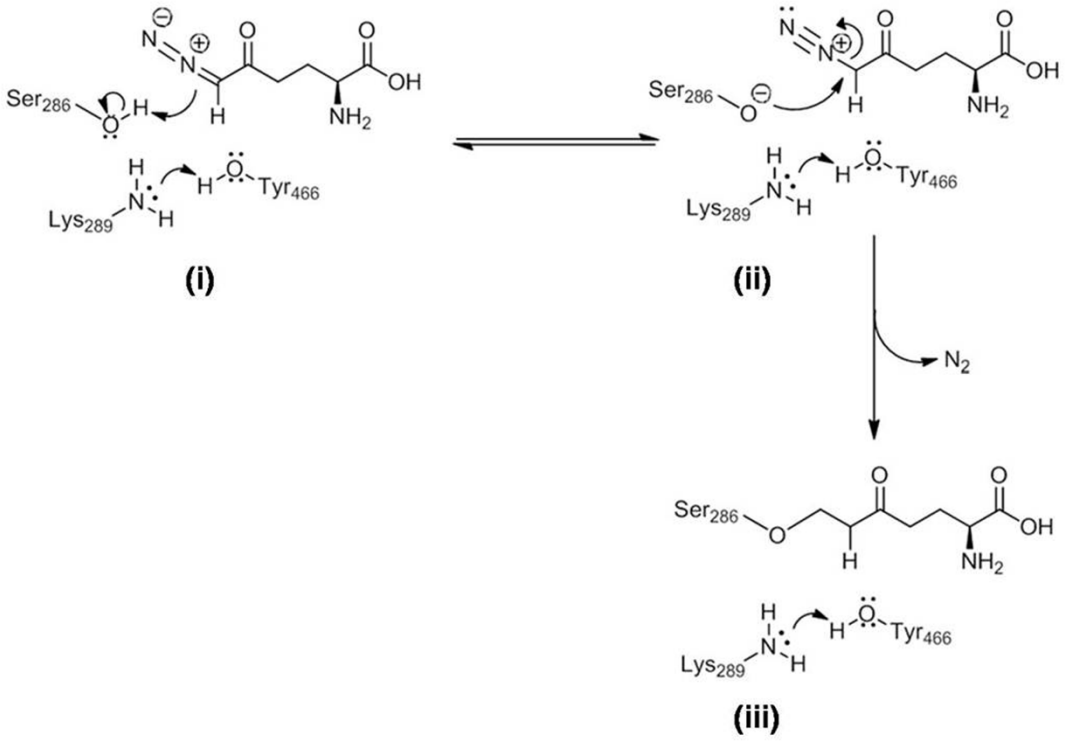

Figure 6 | Proposed active site inhibition mechanism of KGA. The reaction mechanism progresses as follows: (i) Nucleophilic attack of Ser286 on DON; (ii) generation of covalent linkage between Ser286 and DON and the subsequent release of N_2; (iii) formation of acetyl-inhibitor complex.

activity[8]. Furthermore, it was recently proposed that lysine (Lys 316) acetylation in the key loop is important for the regulation and activation of glutaminase[32].

Glutaminase has been found to be elevated in lymphoma, prostate, glioblastoma, breast and kidney cancer cells[5–8]. It was recently reported that Myc stimulates glutaminase (GAC) expression, which directly increases the levels of glutamine metabolism in PC3 and P493 cell lines as compared with normal cells[6]. Notably, in response to Myc, lymphoma cells have shown about a 10-fold increase in the expression of glutaminase. Similarly it was also shown that Rho GTPase enhances glutaminase (GAC) expression in breast and transformed fibroblast cancer cells[7]. In addition to increasing protein expression levels described in these studies, we have recently shown that Ras/Mek kinase could activate the intrinsic activity of KGA in transformed cancer cells through phosphorylation without altering protein expression levels[8]. When used at 50 μM, nearly all of the KGA activity from in cells overexpressing KGA could be inhibited by BPTES, without causing much cytotoxicity to the cells[8]. Collectively, these observations suggest that glutaminase activity could be differentially regulated in cancer cells through alternate

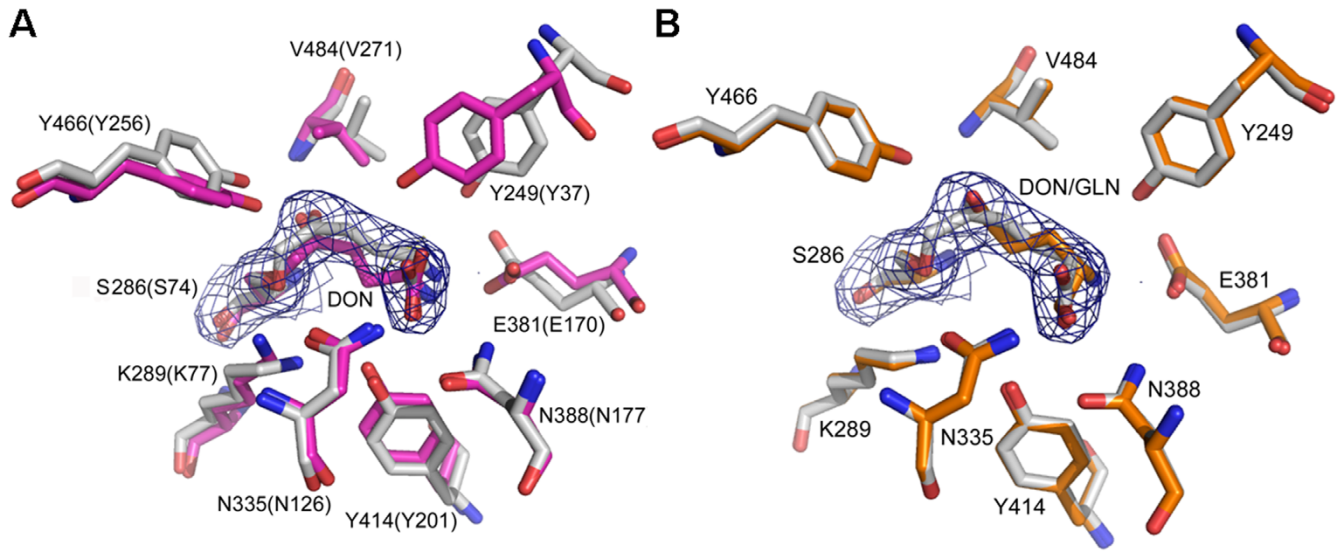

Figure 7 | Structural comparisons. (A) Superposition of cKGA: DON (grey) onto is homolog YbgJ from *B. Subtilis* (PDB code: 3BRM) (magenta). The key active site residues of cKGA are shown, and the equivalent residues from YbgJ are shown in parenthesis. (B) Superposition of cKGA: DON (grey) and the cKGA: Glutamine (PDB code: 3VPO) (orange). The key active site region residues of both complexes of cKGA are shown. DON is shown in the final *2Fo-Fc* electron density map (contoured at 1.0 σ).

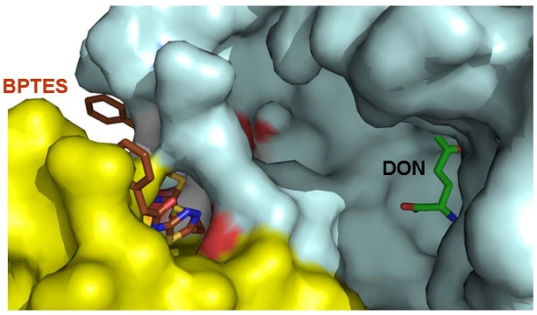

Figure 8 | A model for a proposed hybrid inhibition of KGA combines the actions of BPTES and DON. This model was prepared by superimposing the crystal structure of BPTES: cKGA and DON: cKGA. BPTES binds to the allosteric site, whereas DON binds to the active site region. These two sites are separated by approximately 8 Å, indicating the feasibility of this approach.

mechanisms and the findings point to the urgent need to design a new generation of hybrid inhibitors–with high potency and less toxicity–that selectively inhibit KGA in cancer cells.

To develop better inhibitors that specifically and effectively target KGA, we propose a strategy that targets both the allosteric site and the active site of KGA. This potential new inhibitor could combine optimised derivatives of both BPTES and DON connected via a flexible linker and acts to inhibit KGA by the mechanisms of each inhibitor. This approach is feasible, as the binding sites of these two inhibitors are approximately 8 Å away, as shown in our inhibition model generated using the independent BPTES (allosteric) and DON (active site) (Figure 8). This hybrid inhibitor has the advantage of retaining the specificity of BPTES and simultaneously targeting the active site and allosteric site. Besides, this strategy of inhibition could help to improve the pharmacophore properties and lead to the development of a group of next-generation inhibitors of glutaminase (KGA) with greater potency against KGA, with reduced toxic effects.

Methods

Expression and purification of cKGA. Human cKGA was purified following the procedures described previously[8]. Briefly, cKGA (Ile221-Leu533) was cloned into Pet-28(b) vector and *Escherichia coli* BL21 (DE3)-RIL-Codon plus cells were used to express the protein. The protein was purified using Ni-NTA affinity columns followed by gel filtration chromatography. The buffer conditions were 20 mM Na-Hepes pH 7.5, 200 mM NaCl, 10% glycerol and 2 mM DTT. DON (6-diazo-5-oxo-L-norleucine, NSC 7365), azaserine (*O*-diazoacetyl-L-serine, NSC 742), Glufosinate Ammonium, and L-Methionine Sulfoximine were purchased from Sigma-Aldrich (St. Louis, MO, USA).

Glutaminase assay. A glutaminase assay was performed using the two-step assay described previously[8,33]. Briefly, 10 µL of wild-type cKGA or cKGA harbouring alanine mutations was incubated at 37°C for 10 min with 10 µL of assay mix consisting of 20 mM glutamine, 50 mM Tris·acetate (pH 8.6), 100 mM phosphate, and 0.2 mM EDTA. The reaction was quenched with the addition of 2 µL of 3 M HCl. Subsequently, the reaction mixture was incubated for 30 min at room temperature with 200 µL of the second assay mix (2.2 U glutamate dehydrogenase, 80 mM Tris·acetate (pH 9.4), 200 mM hydrazine, 0.25 mM ADP, and 2 mM nicotinamide adenine dinucleotide). The absorbance was read at 340 nm using a microplate reader (SpectraMax 340; Molecular Devices, Sunnyvale, CA, USA).

Crystallization and data collection. Crystallization screening was carried out by hanging drop vapour diffusion at 22°C. Prior to crystallization, the complex was prepared by incubating approximately 20 mg/mL of cKGA with 10 mM DON (approximately 1 : 10 molar ratio) for 30 min at 4°C. The crystallization drop consisted of 1 µl cKGA: DON complex and 1 µl of the crystallization solution from the reservoir well. The cKGA: DON crystals grew after 2 days in the presence of a solution comprising 0.1 M Bis-Tris propane (pH 7.2) and 1.8 M $LiSO_4$. For the diffraction studies, crystals were cryo-protected with reservoir solution supplemented with 15% glycerol as a cryo-protectant and flash-frozen in liquid nitrogen. Diffraction data were collected at the synchrotron beam line 13B1 (wavelength 1.000 Å) at the National Synchrotron Radiation Research Centre (NSRRC, Taiwan). Data sets were processed and scaled using HKL2000[34]. The crystallographic statistics are provided in Table 1.

Structure solution and refinement. The structure of cKGA-DON complex was determined by molecular replacement with the program MolRep[35] using the coordinates of *apo* cKGA as the search model (Protein data bank, 3VOY)[8]. One molecule of cKGA: DON complex was observed in the asymmetric unit and the initial R-factor was 39%. The model was examined and built in COOT[36] and subsequent refinement was carried out with Phenix-refine[37]. Fitting of the inhibitor and refinements were performed in COOT and Phenix programs, respectively. The final structure was refined up to 2.3 Å resolution with an R-factor of 0.19 (R_{free} 0.21) (Table 1). The overall geometry of the final model was analysed by Ramachandran plot with the program PROCHECK[38].

Site-directed mutagenesis of cKGA. To create all structure-guided mutants of cKGA, we performed site-directed mutagenesis using a kit from Kapa Biosystems, Inc. (Woburn, MA, USA). cKGA cloned into the PET-28(b) vector was used as a template for mutagenesis. Key residues (Tyr249, Ser286, Lys289, and Tyr466) of cKGA were mutated to Ala as a single-point substitution. All mutations were verified by DNA sequencing. Plasmids containing the point mutations were transformed into the *E. coli* BL21 (DE3) RIL strain and the mutant cKGA proteins were over-expressed and purified following the same procedure as the wild-type cKGA.

Protein data bank accession code. Coordinates and structure factors of cKGA: DON complex have been deposited with RCSB Protein Data Bank under access code 407D.

1. Bensinger, S. J. & Christofk, H. R. New aspects of the Warburg effect in cancer cell biology. *Semin Cell Dev Biol* **23**, 352–361 (2012).
2. DeBerardinis, R. J., Lum, J. J., Hatzivassiliou, G. & Thompson, C. B. The biology of cancer: metabolic reprogramming fuels cell growth and proliferation. *Cell Metab* **7**, 11–20 (2008).
3. Rajagopalan, K. N. & DeBerardinis, R. J. Role of glutamine in cancer: therapeutic and imaging implications. *J Nucl Med* **52**, 1005–1008 (2011).
4. DeBerardinis, R. J. & Cheng, T. Q's next: the diverse functions of glutamine in metabolism, cell biology and cancer. *Oncogene* **29**, 313–324 (2010).
5. Seltzer, M. J. *et al.* Inhibition of glutaminase preferentially slows growth of glioma cells with mutant IDH1. *Cancer Res* **70**, 8981–8987 (2010).
6. Gao, P. *et al.* c-Myc suppression of miR-23a/b enhances mitochondrial glutaminase expression and glutamine metabolism. *Nature* **458**, 762–765 (2009).
7. Wang, J. B. *et al.* Targeting mitochondrial glutaminase activity inhibits oncogenic transformation. *Cancer Cell* **18**, 207–219 (2010).
8. Thangavelu, K. *et al.* Structural basis for the allosteric inhibitory mechanism of human kidney-type glutaminase (KGA) and its regulation by Raf-Mek-Erk signaling in cancer cell metabolism. *Proc Natl Acad Sci U S A* **109**, 7705–7710 (2012).
9. Aledo, J. C., Gomez-Fabre, P. M., Olalla, L. & Marquez, J. Identification of two human glutaminase loci and tissue-specific expression of the two related genes. *Mamm Genome* **11**, 1107–1110 (2000).
10. Curthoys, N. P. & Watford, M. Regulation of glutaminase activity and glutamine metabolism. *Annu Rev Nutr* **15**, 133–159 (1995).
11. Andratsch, M. *et al.* TGF-beta signaling and its effect on glutaminase expression in LLC-PK1-FBPase+ cells. *Am J Physiol Renal Physiol* **293**, F846–853 (2007).
12. Hu, W. *et al.* Glutaminase 2, a novel p53 target gene regulating energy metabolism and antioxidant function. *Proc Natl Acad Sci U S A* **107**, 7455–7460 (2010).
13. Suzuki, S. *et al.* Phosphate-activated glutaminase (GLS2), a p53-inducible regulator of glutamine metabolism and reactive oxygen species. *Proc Natl Acad Sci U S A* **107**, 7461–7466 (2010).
14. Shapiro, R. A., Clark, V. M. & Curthoys, N. P. Inactivation of rat renal phosphate-dependent glutaminase with 6-diazo-5-oxo-L-norleucine. Evidence for interaction at the glutamine binding site. *J Biol Chem* **254**, 2835–2838 (1979).
15. Kisner, D. L., Catane, R. & Muggia, F. M. The rediscovery of DON (6-diazo-5-oxo-L-norleucine). *Recent Results Cancer Res* **74**, 258–263 (1980).
16. Ortlund, E., Lacount, M. W., Lewinski, K. & Lebioda, L. Reactions of Pseudomonas 7A glutaminase-asparaginase with diazo analogues of glutamine and asparagine result in unexpected covalent inhibitions and suggests an unusual catalytic triad Thr-Tyr-Glu. *Biochemistry* **39**, 1199–1204 (2000).
17. Pinkus, L. M. Glutamine binding sites. *Methods Enzymol* **46**, 414–427 (1977).
18. Ahluwalia, G. S., Grem, J. L., Hao, Z. & Cooney, D. A. Metabolism and action of amino acid analog anti-cancer agents. *Pharmacol Ther* **46**, 243–271 (1990).
19. Ovejera, A. A., Houchens, D. P., Catane, R., Sheridan, M. A. & Muggia, F. M. Efficacy of 6-diazo-5-oxo-L-norleucine and N-[N-gamma-glutamyl-6-diazo-5-oxo-norleucinyl]-6-diazo-5-oxo-norleucine against experimental tumors in conventional and nude mice. *Cancer Res* **39**, 3220–3224 (1979).
20. Shapiro, R. A., Clark, V. M. & Curthoys, N. P. Covalent interaction of L-2-amino-4-oxo-5-chloropentanoic acid with rat renal phosphate-dependent glutaminase. Evidence for a specific glutamate binding site and of subunit heterogeneity. *J Biol Chem* **253**, 7086–7090 (1978).
21. Brown, G. *et al.* Functional and structural characterization of four glutaminases from Escherichia coli and Bacillus subtilis. *Biochemistry* **47**, 5724–5735 (2008).
22. DeLaBarre, B. *et al.* Full-length human glutaminase in complex with an allosteric inhibitor. *Biochemistry* **50**, 10764–10770 (2011).
23. Cassago, A. *et al.* Mitochondrial localization and structure-based phosphate activation mechanism of Glutaminase C with implications for cancer metabolism. *Proc Natl Acad Sci U S A* **109**, 1092–1097 (2012).

24. Barclay, R. K. & Phillipps, M. A. Effects of 6-diazo-5-oxol-norleucine and other tumor inhibitors on the biosynthesis of nicotinamide adenine dinucleotide in mice. *Cancer Res* **26**, 282–286 (1966).
25. Gill, H. S. & Eisenberg, D. The crystal structure of phosphinothricin in the active site of glutamine synthetase illuminates the mechanism of enzymatic inhibition. *Biochemistry* **40**, 1903–1912 (2001).
26. Liaw, S. H. & Eisenberg, D. Structural model for the reaction mechanism of glutamine synthetase, based on five crystal structures of enzyme-substrate complexes. *Biochemistry* **33**, 675–681 (1994).
27. Garber, K. Oncology's energetic pipeline. *Nat Biotechnol* **28**, 888–891 (2010).
28. Sun, Q. *et al.* Structural basis for the inhibition mechanism of human cystathionine gamma-lyase, an enzyme responsible for the production of H(2)S. *J Biol Chem* **284**, 3076–3085 (2009).
29. Shijie, J. *et al.* Blockade of glutamate release from microglia attenuates experimental autoimmune encephalomyelitis in mice. *Tohoku J Exp Med* **217**, 87–92 (2009).
30. Thomas, A. G. *et al.* Kinetic characterization of ebselen, chelerythrine and apomorphine as glutaminase inhibitors. *Biochem Biophys Res Commun* **438**, 243–248 (2013).
31. Hartman, S. C. & McGrath, T. F. Glutaminase A of escherichia coli. Reactions with the substrate analogue, 6-diazo-5-oxonorleucine. *J Biol Chem* **248**, 8506–8510 (1973).
32. Ferreira, A. P. *et al.* Active glutaminase C self-assembles into a supratetrameric oligomer that can be disrupted by an allosteric inhibitor. *J Biol Chem* **288**, 28009–28020 (2013).
33. Kenny, J. *et al.* Bacterial expression, purification, and characterization of rat kidney-type mitochondrial glutaminase. *Protein Expr Purif* **31**, 140–148 (2003).
34. Otwinowski, Z. & Minor, W. Processing of X-ray diffraction data collected in oscillation mode. *Macromolecular Crystallography, Pt A* **276**, 307–326 (1997).
35. Vagin, A. & Teplyakov, A. Molecular replacement with MOLREP. *Acta Crystallogr D Biol Crystallogr* **66**, 22–25 (2010).
36. Emsley, P. & Cowtan, K. Coot: model-building tools for molecular graphics. *Acta Crystallogr D Biol Crystallogr* **60**, 2126–2132 (2004).
37. Adams, P. D. *et al.* PHENIX: a comprehensive Python-based system for macromolecular structure solution. *Acta Crystallogr D Biol Crystallogr* **66**, 213–221 (2010).
38. Laskowski, R. A., Macarthur, M. W., Moss, D. S. & Thornton, J. M. Procheck - a Program to Check the Stereochemical Quality of Protein Structures. *Journal of Applied Crystallography* **26**, 283–291 (1993).
39. DeLano, W. L. & Lam, J. W. PyMOL: A communications tool for computational models. *Abstracts of Papers of the American Chemical Society* **230**, U1371–U1372 (2005).

Acknowledgments

We are grateful to the Biomedical Research Council of Singapore (BMRC), A*STAR (R154000461305) for the funding support. The X-ray diffraction data for this study were collected at the synchrotron beamline 13B1 at the National Synchrotron Radiation Research Centre (NSRRC, Taiwan). KT is a graduate scholar in receipt of a research scholarship from the National University of Singapore.

Author contributions

J.S. conceived of the study. K.T. carried out crystallographic experiments. K.T. and J.S. analyzed the data. K.T. and Q.Y.C. performed mutation and kinetic experiments. L.B.C. was involved in the analysis. K.T. and J.S. wrote the manuscript with input from all authors.

Additional information

Competing financial interests: The authors declare no competing financial interests.

How to cite this article: Thangavelu, K., Chong, Q.Y., Low, B.C. & Sivaraman, J. Structural Basis for the Active Site Inhibition Mechanism of Human Kidney-Type Glutaminase (KGA). *Sci. Rep.* **4**, 3827; DOI:10.1038/srep03827 (2014).